Polymer Chemistry

Accepted Manuscript

ROYAL SOCIETY OF CHEMISTRY

www.rsc.org/polymers

Cite this: DOI: 10.1039/c0xx00000x

www.rsc.org/xxxxxx

ARTICLE TYPE

Doubly thermo-responsive nanoparticles constructed with two diblock copolymers prepared through two macro-RAFT agents co-mediated dispersion RAFT polymerization

Quanlong Li, Xin He, Yongliang Cui, Pengfei Shi, Shentong Li and Wangqing Zhang*

Received (in XXX, XXX) Xth XXXXXXXXX 20XX, Accepted Xth XXXXXXXXX 20XX
DOI: 10.1039/b000000x

Abstract. A new strategy to prepare doubly thermo-responsive nanoparticles constructed with two diblock copolymers of poly(*N*-isopropylacrylamide)-*block*-polystyrene (PNIPAM-*b*-PS) and poly[*N*,*N*-(dimethylamino) ethyl methacrylate]-*block*-polystyrene (PDMAEMA-*b*-PS) through the two macro-RAFT agents co-mediated dispersion polymerization is proposed. In this two macro-RAFT agents co-mediated dispersion polymerization, two macro-RAFT agents are simultaneously adopted, and two *in situ* synthesized diblock copolymers of PNIPAM-*b*-PS and PDMAEMA-*b*-PS co-assemble into nanoparticles containing a PNIPAM/PDMAEMA mixed corona and a common PS core. It is found that the molecular weight of PNIPAM-*b*-PS and PDMAEMA-*b*-PS in the mixed corona-core nanoparticles increases with the monomer conversion, and the size of mixed corona-core nanoparticles increases with the PS block extension during the two macro-RAFT agents co-mediated dispersion polymerization. In water, the mixed corona-core nanoparticles exhibit two separate phase transition temperatures at 44 ^{o}C and 56 ^{o}C corresponding to the PNIPAM and PDMAEMA blocks, respectively, which is confirmed by turbidity analysis, ^{1}H NMR analysis and TEM observation. The strategy of the two macro-RAFT agents co-mediated dispersion polymerization is believed to be a valid method to prepare multi thermo-responsive nano-objects constructed with two or more than two thermo-responsive diblock copolymers.

1 Introduction

In recent years, thermo-responsive block copolymer nano-objects have aroused great attention because of their potential use in drug delivery, biological separation and tissue engineering scaffolds.[1,2] Of all the thermo-responsive block copolymer nano-objects, the doubly thermo-responsive ones contain two thermo-responsive blocks are interesting.[3-13] Based on the topology of block copolymers, four kinds of doubly thermo-responsive block copolymer nanoparticles as shown in Scheme 1 are generally clarified. In the first case of the linear ABC or BAC triblock terpolymer (note: A and B represent the two thermo-responsive blocks and C represents the solvophobic block throughout this article), two thermo-responsive blocks of A and B locate at the same side of the solvophobic core-forming C block, and the triblock terpolymer nanoparticles have corona-core structure. At the second case of the linear ACB triblock terpolymer, the thermo-responsive A block locates at one side and the thermo-responsive B block locates at the other side of the central solvophobic core-forming C block, and the corona-core nanoparticles have a mixed A/B corona. At the third case of the ABC or BAC miktoarm terpolymer, the two thermo-responsive blocks of A and B are joined at the same terminal of the core-forming C block. At the last case, the nanoparticles are constructed with two thermo-responsive diblock copolymers of AC and BC, in which the C block coming from both AC and BC forms the core and the two thermo-responsive blocks of A and B form the mixed corona.

Up to now, most research is focused on the doubly thermo-responsive nano-objects of ABC and ACB triblock terpolymer through its micellization in the selective solvent for the A and B blocks,[3,4] and no example on the doubly thermo-responsive nano-objects of ABC or BAC miktoarm terpolymer is reported, possibly due to the difficult or laborious synthesis of such complex structure. Compared with ABC triblock terpolymers or ABC miktoarm terpolymers,[3,4,14-19] thermo-responsive AC or BC diblock copolymers can be conveniently prepared.[20-23] However, preparation of well-defined nanoparticles constructed with two diblock copolymers of AC and BC by co-micellization or blending of AC and BC diblock copolymers is not an easy thing,[24-38] since this strategy unavoidably leads to nonergodic micelles constructed with one block copolymer.[38] Besides, since the micelle exchange dynamics is generally very slow due to the high polymer molecular weight,[35-38] translating nonergodic micelles into mixed micelles by inter-micelle macromolecular exchange is very difficult. Thus, it is necessary to discover a convenient synthesis of well-defined doubly thermo-responsive block copolymer nano-objects.

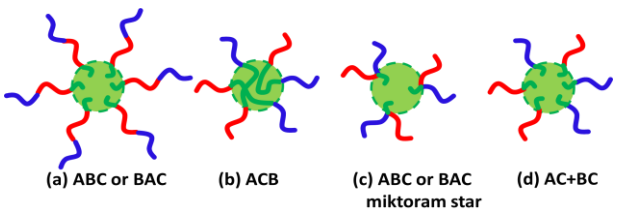

Scheme 1. Summary of doubly thermo-responsive block copolymer nanoparticles.

The macromolecular RAFT (macro-RAFT) agent mediated dispersion polymerization is demonstrated to be a valid method to prepare block copolymer nano-objects.[39-50] Following this method, a soluble macro-RAFT agent, initiator and monomer are one-pot added, and polymerization under dispersion condition is performed, and block copolymer nano-objects with polymer concentration up to 30% can be prepared. Recently, we have prepared doubly thermo-responsive ABC triblock terpolymer nanoparticles of poly(*N*-isopropylacrylamide)-*block*-poly[*N*,*N*-(dimethylamino) ethyl methacrylate]-*block*-polystyrene and poly[poly(ethylene glycol) methyl ether vinylphenyl]-*block*-poly(*N*-isopropylacrylamide)-*block*-polystyrene by dispersion RAFT polymerization,[3,4] which show two separate phase transition temperatures (PTTs) in water. In this contribution, we focus on the convenient preparation of doubly thermo-responsive nanoparticles constructed with two diblock copolymers through a new strategy named the two macro-RAFT agents co-mediated dispersion polymerization. Different from the general macro-RAFT agent mediated dispersion polymerization,[3,4,39-50] two different thermo-responsive macro-RAFT agents, poly(*N*-isopropylacrylamide) trithiocarbonate (PNIPAM-TTC) and poly[*N*,*N*-(dimethylamino) ethyl methacrylate] trithiocarbonate (PDMAEMA-TTC), are simultaneously adopted in the dispersion RAFT polymerization. This two macro-RAFT agents co-mediated dispersion polymerization affords simultaneous synthesis of two thermo-responsive diblock copolymers of poly(*N*-isopropylacrylamide)-*block*-polystyrene (PNIPAM-*b*-PS) and poly[*N*,*N*-(dimethylamino) ethyl methacrylate]-*block*-polystyrene) (PDMAEMA-*b*-PS) and their co-assembly into nanoparticles containing a mixed corona of PNIPAM/PDMAEMA and a PS core, which exhibit two separate PTTs at 44 ^{o}C and 56 ^{o}C in water.

2 Experimental

2.1 Materials

The monomer of *N*-isopropylacrylamide (NIPAM, >99%, Acros Organics) was purified by recrystallization in the acetone/*n*-hexane mixture (50:50 by volume). The monomer of *N*,*N*-(dimethylamino) ethyl methacrylate (DMAEMA, 98%, Alfa, Scheme S1) was dried with CaH_2 overnight and distilled under reduced pressure prior to use. Styrene (St, >98%, Tianjin Chemical Company) was distilled under vacuum and stored at -5 ^{o}C prior to use. 2,2'-Azobis(2-methylpropionitrile) (AIBN, >99%, Tianjin Chemical Company) was recrystallized from ethanol before being used. The RAFT agent of 4-cyano-4-(dodecylsulfanylthiocarbonyl) sulfanyl pentanoic acid (CDTPA, Scheme S1) was synthesized as discussed elsewhere.[51] Other chemical reagents were analytic grade and were used as received. Deionized water was used in the present experiments.

2.2 Synthesis of PNIPAM-TTC

The PNIPAM-TTC macro-RAFT agent was synthesized by solution RAFT polymerization. Into a 100 mL Schlenk flask with a magnetic bar, NIPAM (10.0 g, 88.4 mmol), CDTPA (356.7 mg, 0.88 mmol), and AIBN (36.3 mg, 0.22 mmol) dissolved in 1,4-dioxane (35.0 g) were added. The solution was degassed with nitrogen at 0 ^{o}C, and then the flask content was immersed into preheated oil bath at 65 ^{o}C for 150 min. The polymerization was quenched by rapid cooling upon immersion of the flask in iced water. The monomer conversion of 92% was determined by ^{1}H NMR analysis. The synthesized polymer was precipitated in iced diethyl ether, and then dried under vacuum at room temperature overnight to afford yellow powder of PNIPAM-TTC (8.4 g, 87% yield).

2.3 Synthesis of PDMAEMA-TTC

The PDMAEMA-TTC macro-RAFT agent was synthesized by RAFT polymerization in 1,4-dioxane using AIBN as initiator and CDTPA as RAFT agent. Into a 50 mL Schlenk flask with a magnetic bar, DMAEMA (10.0 g, 6.37 mmol), CDTPA (0.321 g, 0.80 mmol), and AIBN (16.4 mg, 0.10 mmol) dissolved in 1,4-dioxane (10.0 g) were added. The solution was degassed with nitrogen at 0 ^{o}C, and then the flask content was immersed into preheated oil bath at 70 ^{o}C for 4.5 h. The polymerization was quenched by rapid cooling upon immersion of the flask in iced water. To detect the monomer conversion, a drop of the polymerization solution was dropped into $CDCl_3$ and subjected to ^{1}H NMR analysis. The monomer conversion at 61% was calculated by comparing the integral areas of the protons of the double-bond peaks at δ = 5.56 ppm in reference to the protons peaks of the methylene at δ = 4.07 ppm. To collect the polymer, the flask content was precipitated in *n*-hexane at 0 ^{o}C, dried under vacuum at room temperature overnight to afford yellow powder of PDMAEMA-TTC (5.5 g, 53% yield).

2.4 Two macro-RAFT agents co-mediated dispersion polymerization and synthesis of mixed corona-core nanoparticles

The two macro-RAFT agents co-mediated dispersion polymerization of styrene was performed in the 85/15 methanol/water mixture at 70 ^{o}C under $[St]_0$:$[PNIPAM\text{-}TTC]_0$:$[PDMAEMA\text{-}TTC]_0$:$[AIBN]_0$ = 1800:3:3:1 with a constant weight ratio of the fed styrene monomer to the solvent at 15%. Into a Schlenk flask with a magnetic bar, PDMAEMA-TTC (0.200 g, 0.020 mmol), PNIPAM-TTC (0.219 g, 0.020 mmol), St (1.250 g, 12.0 mmol), and AIBN (1.10 mg, 0.0066 mmol) dissolved in the 85/15 methanol/water mixture (8.32 g) were added. The solution was degassed with nitrogen at 0 ^{o}C, and then the polymerization was performed at 70 ^{o}C under vigorous stirring. After a given time, the polymerization was quenched by rapid cooling upon immersion of the flask in iced water to afford the mixed corona-core nanoparticles constructed with two diblock copolymers of PNIPAM-*b*-PS/PDMAEMA-*b*-PS.

The monomer conversion in the two macro-RAFT agents co-mediated dispersion polymerization was detected by UV-vis analysis at 245 nm as discussed elsewhere.[49] To remove the residual St monomer in the colloidal dispersion, the colloidal dispersion was dialyzed against water at room temperature (20-25 ^{o}C) for three days (molecular weight cutoff: 7000 Da) to afford the aqueous dispersion of the mixed corona-core nanoparticles of PNIPAM-*b*-PS/PDMAEMA-*b*-PS (the polymer concentration at 1-10 wt% dependent on the monomer conversion). To collect the polymer for further gel permeation chromatography (GPC) analysis and ^{1}H NMR analysis, part of the aqueous colloidal dispersion was extracted with dichloromethane, and then the organic phase was collected and dried over anhydrous magnesium sulfate overnight. After filtration of magnesium

sulfate and removal of the solvent, the polymer was collected and dried under vacuum at room temperature overnight to afford pale yellow powder of the PNIPAM-*b*-PS/PDMAEMA-*b*-PS mixture.

2.5 Characterizations

The GPC analysis was performed on a Waters 600E GPC system equipped with three TSK-GEL columns and a Waters 2414 refractive index detector, where THF containing 3 wt% triethylamine was used as eluent at flow rate of 0.5 mL/min at 30.0 °C and the narrow-polydispersity polystyrene (molecular weight: 500-280500 Da) was used as calibration standard, from which the polymer molecular weight M_n and M_w or its distribution $Đ$ ($Đ = M_w/M_n$) were obtained. The triethylamine in the eluent of THF was to reduce the interaction of the N-containing polymer with the GPC columns as discussed elsewhere.[52] The ^{1}H NMR analysis was performed on a Bruker Avance III 400MHz NMR spectrometer. For polymers dissolved in $CDCl_3$, the proton signal at δ = 7.26 ppm of the internal solvent was used as standard; and for polymers dissolved in D_2O, the chemical shift of 1,3,5-trioxane at δ = 5.20 ppm was locked and the signal was used as reference. The styrene monomer conversion in the dispersion RAFT polymerization was determined by UV-vis analysis, in which a given volume of the colloidal dispersion (1.0 mL) was filtrated twice with a 0.22 μm nylon filter, diluted with alcohol, and analysed by UV-vis analysis at 245 nm. The PTT of the thermo-responsive polymers was determined by turbidity analysis at 500 nm on a Varian 100 UV-vis spectrophotometer equipped with a thermo-regulator (± 0.1 °C) with the heating rate at 1 °C/min. The PTT was determined at the middle point of the transmittance change. The transmission electron microscopy (TEM) observation was performed using a Tecnai G^2 F20 electron microscope at an acceleration of 200 kV, whereby a small drop of the preheated dispersion of the synthesized nanoparticles was dripped onto a piece of preheated copper grid till the solvent was evaporated at a given temperature.

3 Results and discussion

3.1 Synthesis of the PNIPAM-TTC and PDMAEMA-TTC macro-RAFT agents

The PNIPAM-TTC macro-RAFT agent was synthesized by solution RAFT polymerization of NIPAM in 1,4-dioxane under $[NIPAM]_0$:$[CDTPA]_0$:$[AIBN]_0$ = 400:4:1. The solution RAFT polymerization of NIPAM runs smoothly and 92% monomer conversion was achieved in 150 min. The synthesized PNIPAM-TTC was characterized by ^{1}H NMR analysis (Figure 1A) and GPC analysis (Figure 2). Based on the proton resonance signals at δ = 0.88 ppm corresponding to the RAFT agent terminal and δ = 4.00 ppm corresponding to the polymer main chains shown in Figure 1A, the molecular weight $M_{n,NMR}$ of the synthesized PNIPAM-TTC at 9.6 kg/mol is calculated. The molecular weight $M_{n,GPC}$ of PNIPAM-TTC by GPC analysis is 6.4 kg/mol, and the molecular weight is narrowly dispersed with $Đ$ = 1.24. It is found that, $M_{n,NMR}$ of PNIPAM-TTC is very close to the theoretical molecular weight $M_{n,th}$, which is 10.9 kg/mol calculated by the monomer conversion following eqn 1 as described elsewhere.[53] In the next discussion, PNIPAM-TTC is labeled as $PNIPAM_{92}$-TTC, in which the polymerization degree (DP) is determined by $M_{n,th}$.

The PDMAEMA-TTC macro-RAFT agent was synthesized by the RAFT polymerization of DMAEMA in 1,4-dioxane using CDTPA as RAFT agent and AIBN as initiator. The PDMAEMA-TTC macro-RAFT agent was also characterized by ^{1}H NMR analysis (Figure 1B) and GPC analysis (Figure 2). The molecular weight $M_{n,NMR}$ of the PDMAEMA-TTC macro-RAFT agent, 8.7 kg/mol, is calculated by comparing the proton resonance signals at δ = 4.07 ppm and δ = 1.26 ppm. The molecular weight $M_{n,GPC}$ of PDMAEMA-TTC by GPC analysis is 12.5 kg/mol, and the molecular weight narrowly dispersed with $Đ$ = 1.15. It is found that, the molecular weight $M_{n,NMR}$ of PDMAEMA-TTC by ^{1}H NMR analysis is close to $M_{n,th}$, which is 10.0 kg/mol calculated by the monomer conversion following eqn 1, and $M_{n,GPC}$ is larger than $M_{n,th}$. The slight difference in $M_{n,NMR}$, $M_{n,GPC}$ and $M_{n,th}$ is possibly ascribed to the non-polar polystyrene standard employed in the GPC analysis. In the next discussion, PDMAEMA-TTC is labeled as $PDMAEMA_{61}$-TTC, in which the DP is determined by $M_{n,th}$.

$$M_{n,th} = \frac{[\text{monomer}]_0 \times M_{monomer}}{[\text{RAFT}]_0} \times conversion + M_{RAFT} \quad (1)$$

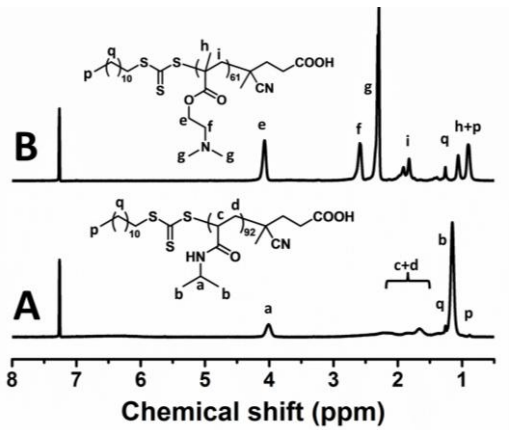

Figure 1. The ^{1}H NMR spectra of $PNIPAM_{92}$-TTC (A) and $PDMAEMA_{61}$-TTC (B).

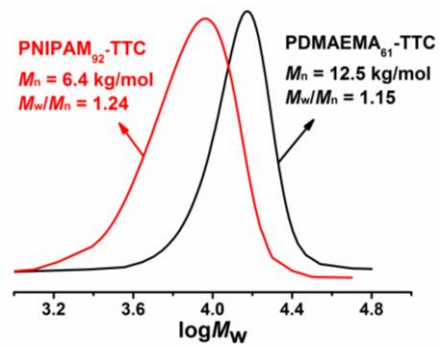

Figure 2. The GPC traces of $PNIPAM_{92}$-TTC and $PDMAEMA_{61}$-TTC.

3.2 Two macro-RAFT agents co-mediated dispersion polymerization and synthesis of mixed corona-core nanoparticles

The two macro-RAFT agents co-mediated dispersion

polymerization of styrene was performed in the 85/15 methanol/water mixture under $[St]_0$:$[PNIPAM\text{-}TTC]_0$:$[PDMAEMA\text{-}TTC]_0$:$[AIBN]_0$ = 1800:3:3:1. The solvent of the 85/15 methanol/water mixture was chosen, since it is a good solvent for the two macro-RAFT agents of PNIPAM-TTC and PDMAEMA-TTC and the St monomer but a non-solvent of the PS block, which is essential for the polymerization-induced self-assembly of PNIPAM-*b*-PS/PDMAEMA-*b*-PS. It was optically observed that the dispersion RAFT polymerization underwent an initial homogeneous stage below 4 h and a subsequent heterogeneous stage, which is very similar with the individual macro-RAFT agent mediated dispersion polymerizations reported by Armes and by our research group.[41-49] This two-stage polymerization is due to the PNIPAM-*b*-PS/PDMAEMA-*b*-PS diblock copolymers synthesized in the initial stage being molecularly soluble in the polymerization medium and becoming insoluble with the extension of the solvophobic PS block in the later stage. As shown in Figure 3, the monomer conversion increases steadily in the initial 4 h at the homogenous stage, and increases quickly to 84.3% in 14 h, and then increases slowly to 90.9% when the polymerization extends to 24 h, which is very similar with those in the individual macro-RAFT agent mediated dispersion polymerization under similar conditions (Figure S1). The $\ln([M]_0/[M])$ *vs* polymerization time plot is shown in Figure S2, in which a two-stage plot containing a gradient linear stage corresponding to the initial homogeneous polymerization and a steep linear one corresponding to the later heterogeneous polymerization is observed. This clearly suggests that, the two macro-RAFT agents co-mediated dispersion RAFT polymerization undergoes a similar polymerization kinetics with those in the presence of an individual macro-RAFT agent.

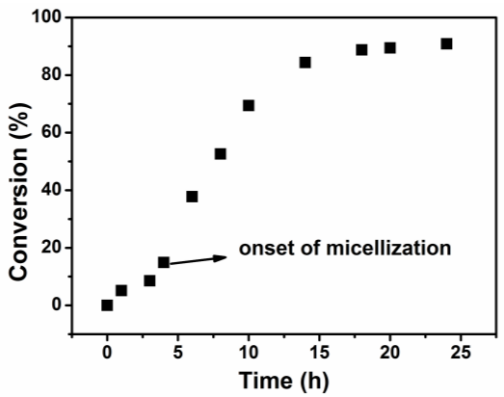

Figure 3. The monomer conversion-time plots for the two macro-RAFT agents co-mediated dispersion polymerization. Polymerization conditions: St (1.250 g, 12.0 mmol), the methanol/water mixture (8.32 g, 80/20 by weight), $[St]_0$:$[PNIPAM\text{-}TTC]_0$:$[PDMAEMA\text{-}TTC]_0$:$[AIBN]_0$ = 1800:3:3:1, 70 °C.

The polymer synthesized through the two macro-RAFT agents co-mediated dispersion polymerization at different polymerization time was characterized by GPC analysis and ^{1}H NMR analysis. From the GPC traces shown in Figure 4, bimodal GPC traces of the synthesized polymer below 8 h of polymerization, unimodal GPC traces after 8 h of polymerization, and a clear shift from low to high molar mass with the increasing monomer conversion are observed. Figure 5 shows the ^{1}H NMR spectra of the typical polymers synthesized at 4 h and 24 h, from which the characteristic chemical shifts due to the PNIPAM block, the PDMAEMA block and the PS block are clearly discerned at the two cases of polymerization time, suggesting formation of two diblock copolymers of PNIPAM-*b*-PS and PDMAEMA-*b*-PS. By checking the GPC traces of the two macro-RAFT agents and the two diblock copolymers of PNIPAM-*b*-PS and PDMAEMA-*b*-PS synthesized in the initial RAFT polymerization, it is deemed that the right peak in the bimodal GPC traces is ascribed to PNIPAM-*b*-PS and the left peak is ascribed to PDMAEMA-*b*-PS. To further clarify which peak in the bimodal GPC traces belonging to PNIPAM-*b*-PS or PDMAEMA-*b*-PS, the separation of the individual diblock copolymer from the PNIPAM-*b*-PS/PDMAEMA-*b*-PS mixture was attempted. Since PDMAEMA and PS are soluble in iced diethyl ether, whereas PNIPAM is insoluble in iced diethyl ether, the separation of diblock copolymers by firstly dissolving the polymer in dichloromethane and then depositing in iced diethyl ether was made (seeing the separation detail in Supporting Information). However, successful separation was not achieved even after several dissolving/precipitation cycles. The unsuccessful separation is possibly due to the co-precipitation of PNIPAM-*b*-PS and PDMAEMA-*b*-PS in iced diethyl ether. Besides, since the PNIPAM-*b*-PS diblock copolymer containing a relatively long PS block is somewhat soluble in iced diethyl ether, which also makes trouble in the separation. However, by comparing the ^{1}H NMR spectra and the GPC traces of the precipitate with those of the PNIPAM-*b*-PS/PDMAEMA-*b*-PS mixture before separation, the weakening signals due to the PDMAEMA-*b*-PS diblock copolymer in both ^{1}H NMR spectra and GPC traces have been detected (Figure S3), and therefore the above speculation is confirmed. Based on the GPC analysis, the molecular weight $M_{n,GPC}$ of the individual diblock copolymer in the PNIPAM-*b*-PS/PDMAEMA-*b*-PS mixture prepared at different polymerization time and the molecular weight distribution, $Đ$, are obtained and summarized in Figure 6. Note: at cases of the unimodal GPC traces, the same molecular weight $M_{n,GPC}$ of PNIPAM-*b*-PS and PDMAEMA-*b*-PS is approximately assumed. It is found that, the molecular weight of PNIPAM-*b*-PS or PDMAEMA-*b*-PS increases with the increasing monomer conversion, which is similarly with those in the individual macro-RAFT agent mediated polymerization.[3,4,39-50]

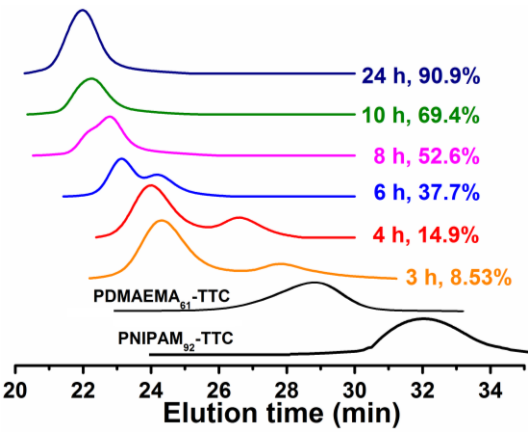

Figure 4. The GPC traces of the synthesized PNIPAM-*b*-PS/PDMAEMA-*b*-PS mixture and the macro-RAFT agents of $PNIPAM_{92}$-TTC and $PDMAEMA_{61}$-TTC.

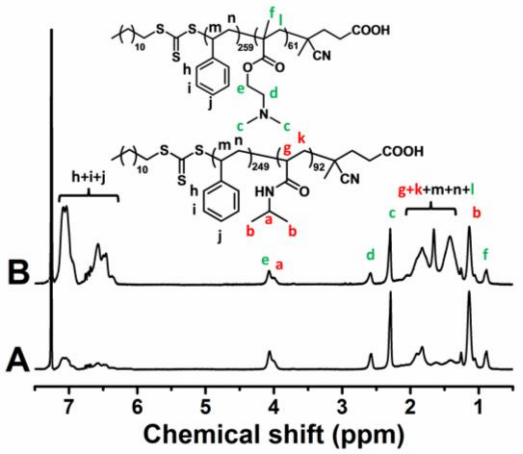

Figure 5. The ^{1}H NMR spectra of the synthesized PNIPAM-*b*-PS/PDMAEMA-*b*-PS mixture at polymerization time of 4 h (A) and 24 h (B).

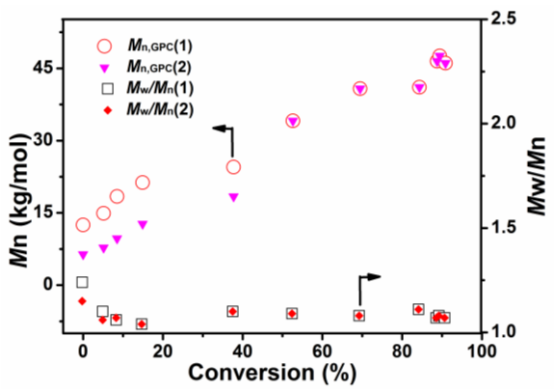

Figure 6. The evolution of the molecular weight $M_{n,GPC}$ and its distribution $Đ$ of PDMAEMA-*b*-PS (1) and PNIPAM-*b*-PS (2) in the PNIPAM-*b*-PS/PDMAEMA-*b*-PS mixture with the monomer conversion in the two macro-RAFT agents co-mediated dispersion polymerization.

Figure 7 shows the TEM images of the mixed corona-core nanoparticles dispersed in water prepared through the two macro-RAFT agents co-mediated dispersion polymerization, from which uniform nanoparticles are observed. By statistical analysis of above 100 particles, the average diameter (D) of the mixed corona-core nanoparticles is obtained and the results are summarized in Figure 8. The results show that the average diameter (D) of the mixed corona-core nanoparticles increases with the polymerization time, which is as similar as those of diblock copolymer nanoparticles in the individual macro-RAFT agent mediated dispersion polymerization.[3,4,46-49] The typical mixed corona-core nanoparticles of $PNIPAM_{92}$-*b*-PS_{273}/$PDMAEMA_{61}$-*b*-PS_{273} are compared with the two nano-objects constructed with one individual diblock copolymer, the $PNIPAM_{92}$-*b*-PS_{275} nanoparticles (Figure S4A) and the $PDMAEMA_{61}$-*b*-PS_{265} nanoparticles (Figure S4B), which were prepared through the individual macro-RAFT agent mediated dispersion polymerization under the other same conditions such as the constant polymerization time of 24 h under $[St]_0$:$[macro\text{-}RAFT]_0$:$[AIBN]_0$ = 1800:6:1. It is found that the three nanoparticles have similar diameter at 32-35 nm. This is not surprised, since the DP of the PS block in the three nanoparticles is very similar with each other.

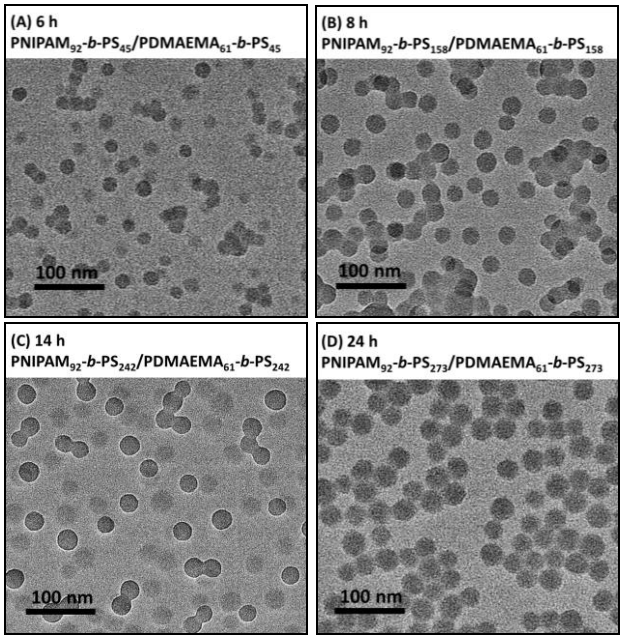

Figure 7. The TEM images of the mixed corona-core nanoparticles of PNIPAM-*b*-PS/PDMAEMA-*b*-PS prepared at polymerization time of 6 h (A), 8 h (B), 14 h (C) and 24 h (D). Insets: the chemical composition of PNIPAM-*b*-PS/PDMAEMA-*b*-PS, in which the DP of the PS block is determined by the monomer conversion by assuming the similar DP in PNIPAM-*b*-PS and PDMAEMA-*b*-PS.

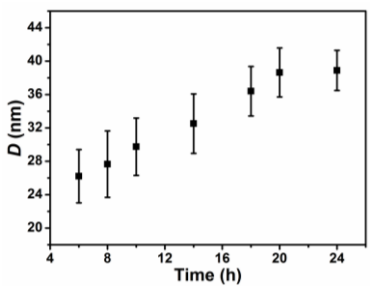

Figure 8. The average size of the mixed corona-core nanoparticles of PNIPAM-*b*-PS/PDMAEMA-*b*-PS prepared through the two macro-RAFT agents co-mediated dispersion polymerization at different polymerization time.

3.3 Double thermo-response of the mixed corona-core nanoparticles

Since the mixed corona-core nanoparticles contain two thermo-responsive blocks of PNIPAM and PDMAEMA, their temperature-sensitive response in water is expected. Figure 9A shows the temperature dependent transmittance of the aqueous dispersion of the typical mixed corona-core nanoparticles of $PNIPAM_{92}$-*b*-PS_{273}/$PDMAEMA_{61}$-*b*-PS_{273}, from which two PTTs at 44 °C and 56 °C have been observed, and therefore the double thermo-response of the mixed corona-core nanoparticles is concluded. By checking the thermo-response of the reference polymers of $PNIPAM_{92}$-TTC and $PDMAEMA_{61}$-TTC (Figure S5), it is concluded that the first PTT at 44 °C is ascribed to the PNIPAM block and the second PTT at 56 °C is ascribed to the PDMAEMA block, respectively. Compared with the soluble-to-insoluble phase transition of the reference polymers of

PNIPAM$_{92}$-TTC at 30 °C and PDMAEMA$_{61}$-TTC at 42 °C, two differences in the thermo-response of the mixed corona-core nanoparticles are detected. First, the PTT of the PNIPAM block and the PDMAEMA block in the mixed corona-core nanoparticles is higher than those of the reference thermo-responsive polymers. Second, the phase transition of the PNIPAM block or the PDMAEMA block in the mixed corona-core nanoparticles occurs within a wide temperature range, *e.g.* 15 °C for the PNIPAM block and 5 °C for the PDMAEMA block, respectively. The reason for the increase in the PTTs of the PNIPAM and PDMAEMA blocks in the mixed corona-core nanoparticles is possibly due to the steric repulsion among the crowded polymer chains tethered on the PS core, which retards the soluble-to-insoluble transition of the tethered PNIPAM and PDMAEMA chains as discussed elsewhere.[54]

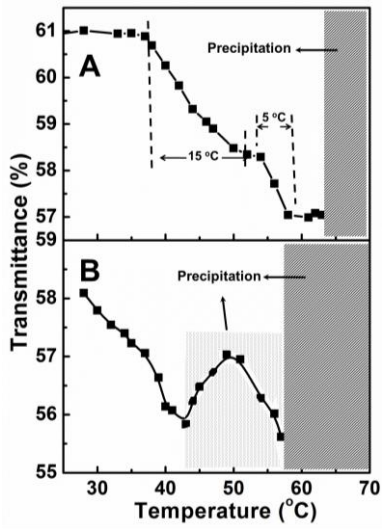

Figure 9. The temperature dependent transmittance of the 0.01 wt% aqueous dispersion of the mixed corona-core nanoparticles of PNIPAM$_{92}$-*b*-PS$_{273}$/PDMAEMA$_{61}$-*b*-PS$_{273}$ (A), and the mixture of two nanoparticles of PNIPAM$_{92}$-*b*-PS$_{275}$ and PDMAEMA$_{61}$-*b*-PS$_{265}$ by simply blending with the weight ratio of the two nanoparticles at 1/1 (B).

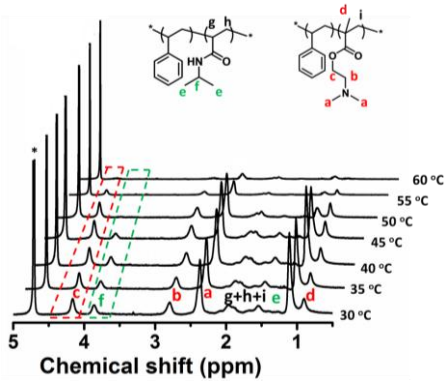

Figure 10. Temperature-dependent ^{1}H NMR spectra of the mixed corona-core nanoparticles of PNIPAM$_{92}$-*b*-PS$_{273}$/PDMAEMA$_{61}$-*b*-PS$_{273}$ dispersed in D_2O (*= D_2O).

The thermo-response of the mixed corona-core nanoparticles of PNIPAM$_{92}$-*b*-PS$_{273}$/PDMAEMA$_{61}$-*b*-PS$_{273}$ is further checked by variable temperature ^{1}H NMR analysis. As shown by the ^{1}H NMR spectra in Figure 10, the proton signals assigned to the PNIPAM and PDMAEMA blocks are clearly discerned at temperature of 35 °C, suggesting both the PNIPAM and PDMAEMA blocks being soluble at this temperature below PTT of the PNIPAM block. Note: the PS block is insoluble in D_2O and very faint signal is detected, and therefore is not discussed herein. When temperature increases from 35 to 50 °C, the gradual decrease of the typical proton signal at δ = 3.86 ppm [f, C***H***$(CH_3)_2$] assigned to the PNIPAM block as indicated by green rectangle in Figure 10 is detected, suggesting the soluble-to-insoluble phase transition of the PNIPAM block. When temperature further increases from 50 to 60 °C, the gradual decrease of the typical proton signal at δ = 4.16 ppm (c, COOC***H***$_2$) assigned to the PDMAEMA block as indicated by red rectangle is detected, suggesting the soluble-to-insoluble phase transition of the PDMAEMA block. These results confirm the two-step phase transition of the PNIPAM block and the PDMAEMA block in the mixed corona-core nanoparticles.

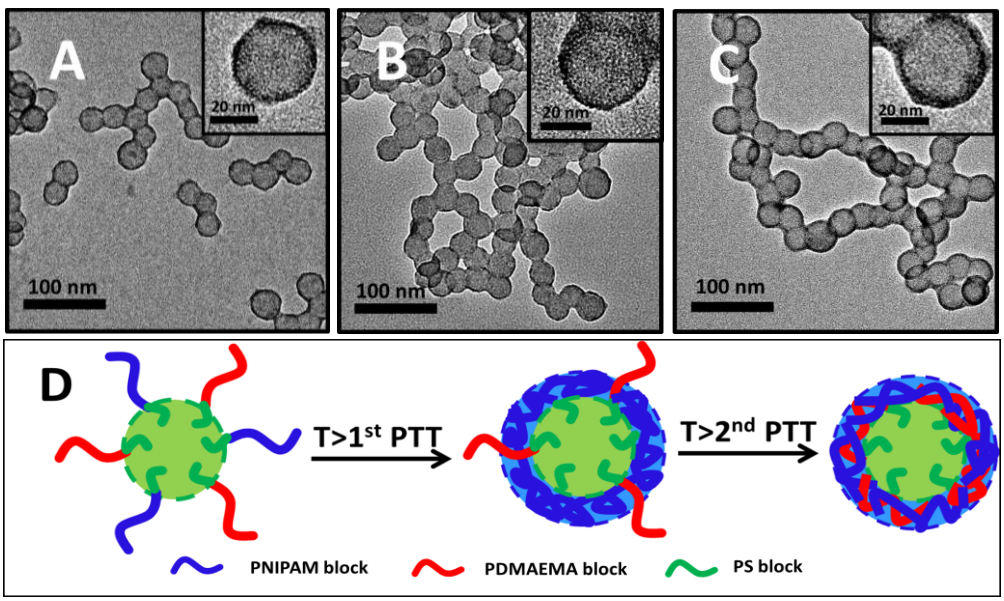

Figure 11. TEM images of the mixed nanoparticles of PNIPAM$_{92}$-*b*-PS$_{273}$/PDMAEMA$_{61}$-*b*-PS$_{273}$ at the temperature of 25 °C (A), 50 °C (B) and 60 °C (C), and the schematic thermo-response of the mixed corona-core nanoparticles dispersed in water upon temperature increasing (D).

The thermo-response of the PNIPAM and PDMAEMA blocks is expected to lead morphology change of the mixed corona-core nanoparticles of $PNIPAM_{92}$-*b*-PS_{273}/$PDMAEMA_{61}$-*b*-PS_{273}. That is, in water at temperature below the first PTT of the PNIPAM block, the PNIPAM and PDMAEMA blocks are soluble, and therefore the nanoparticles contain a solvophobic PS core and a PNIPAM/PDMAEMA mixed corona; at temperature above the first PTT of the PNIPAM block, the PNIPAM block deposits onto the PS core and meanwhile the PDMAEMA block keeps soluble; at temperature above the second PTT of the PDMAEMA block, the PDMAEMA block further deposits onto the PS core, and therefore the nanoparticles contain a solvophobic PS core and the insoluble shell of PNIPAM/PDMAEMA. To detect the morphology change, three samples of the diluted aqueous dispersion of the mixed corona-core nanoparticles were kept at temperature of 25 ^{o}C (below the first PTT), 50 ^{o}C (above the first PTT) and 60 ^{o}C (above the second PTT) for 30 min, and then the morphology of the nanoparticles was checked by TEM. From the TEM images shown in Figure 11, uniform nanoparticles with the diameter at 33 nm (Figure 11A), 35 nm (Figure 11B), and 36 nm (Figure 11C) have been observed at three cases of temperature. Note: the solvophobic core-forming block is visible and the soluble corona-forming block is invisible in the TEM images as discussed elsewhere.[55] This slight increase in the diameter of the nanoparticles possibly suggests the two-step soluble-to-insoluble phase transition of the PNIPAM block and the PDMAEMA block on the PS core. By assuming the dark shell being constructed with the PNIPAM chains or the PNIPAM/PDMAEMA chains and the shell density being equal to the bulk polymer, the shell thickness of the nanoparticles, 1.0 nm at 50 ^{o}C and 1.8 nm at 60 ^{o}C, can be approximately calculated, thus the theoretical diameter of the nanoparticles, 35 nm at 50 ^{o}C (above the first PTT) and 36.6 nm at 60 ^{o}C (above the second PTT), is calculated, which is well consistent with those by TEM. Besides, the slight difference in the thickness of the dark periphery of the nanoparticles, 2 nm at 25 ^{o}C, 3 nm at 50 ^{o}C and 5 nm at 60 ^{o}C, is observed. Note: the dark periphery is ascribed to the deposited PNIPAM or PNIPAM/PDMAEMA chains, since they have relatively higher electron density compared with the PS block. Despite the approximate estimation of the dark periphery of the nanoparticles being seriously affected by the TEM sampling, the increase in the thickness of the dark periphery of the nanoparticles with temperature increasing is concluded. Based on the TEM observation, the thermo-response of the mixed corona-core nanoparticles as schematically shown in Figure 11D is therefore concluded.

Lastly, the thermo-response of the mixed corona-core nanoparticles of $PNIPAM_{92}$-*b*-PS_{273}/$PDMAEMA_{61}$-*b*-PS_{273} is compared with the mixture of the $PNIPAM_{92}$-*b*-PS_{275} nanoparticles and the $PDMAEMA_{61}$-*b*-PS_{265} nanoparticles. This mixture was prepared by blending the two samples of the aqueous dispersion of the $PNIPAM_{92}$-*b*-PS_{275} nanoparticles and the $PDMAEMA_{61}$-*b*-PS_{265} nanoparticles (1:1 by volume and 1/1 by polymer weight), in which the composition of the two diblock copolymers is similar with those in the mixed corona-core nanoparticles. As shown in Figure 9B, the transmittance of the mixture of two diblock copolymer nanoparticles initially decreases from 28 ^{o}C to 43 ^{o}C, which can be ascribed to the phase transition of the PNIPAM block in the $PNIPAM_{92}$-*b*-PS_{273} nanoparticles at PTT of 36 ^{o}C. When the temperature increases from 43 ^{o}C to 49 ^{o}C, the colloids become unstable and little precipitate deposited on the bottom of the glass cell is observed, which leads to the slight increase in the transmittance as shown in Figure 9B. When temperature increases from 49 ^{o}C to 57 ^{o}C, the phase transition of the PDMAEMA block in the $PDMAEMA_{61}$-*b*-PS_{265} nanoparticles takes place and the transmittance decreases again as shown in Figure 9B. The further increase in temperature leads to almost complete precipitation of the nanoparticles. By comparing the thermo-response of the mixed corona-core nanoparticles and the mixture of two individual diblock copolymer nanoparticles, two differences in the thermo-response are observed. First, the PTTs of the PNIPAM block and the PDMAEMA block in the mixed corona-core nanoparticles are higher than those in the mixture of two individual nanoparticles (44 ^{o}C *vs* 36 ^{o}C for the PNIPAM block, and 56 ^{o}C *vs* 53 ^{o}C for the PDMAEMA block). The reason is possibly due to the much crowded corona-forming thermo-responsive chains on the PS core in the mixed corona-core nanoparticles, which makes the phase transition at higher temperature in the mixed corona-core nanoparticles than in the mixture of two individual nanoparticles.[54] Second, the mixed corona-core nanoparticles are more stable than the mixture of two individual nanoparticles at temperature above the PTT of the PNIPAM block. For examples, the mixed corona-core nanoparticles keep suspending in water at temperature above PTT of the PNIPAM block, since the corona-forming PDMAEMA block keeps soluble in water; whereas due to the dehydration of the PNIPAM block at this temperature, part of the $PNIPAM_{92}$-*b*-PS_{275} nanoparticles in the mixture of two individual nanoparticles deposit as shown in Figure 9. The different thermo-response further confirms the mixed corona-core nanoparticles being constructed with two diblock copolymers.

4 Conclusions

Doubly thermo-responsive nanoparticles constructed with two diblock copolymers of PNIPAM-*b*-PS and PDMAEMA-*b*-PS are prepared through the two macro-RAFT agents co-mediated dispersion polymerization. In this two macro-RAFT agents co-mediated dispersion polymerization, two macro-RAFT agents are simultaneously adopted, and two *in situ* synthesized thermo-response diblock copolymers of PNIPAM-*b*-PS and PDMAEMA-*b*-PS are simultaneously co-assembled into mixed nanoparticles constructed with PNIPAM-*b*-PS and PDMAEMA-*b*-PS. It is found that the two macro-RAFT agents co-mediated dispersion polymerization undergoes a polymerization kinetics similarly with the individual macro-RAFT agent mediated dispersion polymerization. The molecular weight of PNIPAM-*b*-PS and PDMAEMA-*b*-PS in the mixed nanoparticles increases with the monomer conversion, and the size of the mixed nanoparticles increases with the PS block extension during the dispersion RAFT polymerization. In water, the mixed nanoparticles have a corona-core structure, in which the PNIPAM and PDMAEMA blocks form the mixed core, and the common PS block in the two diblock copolymers forms the core. The double thermo-response of the mixed corona-core nanoparticles is confirmed by turbidity analysis, ^{1}H NMR analysis and TEM observation. Our strategy of the two macro-RAFT agents co-mediated dispersion

polymerization is believed to be a valid method to prepare multi thermo-responsive nano-objects constructed with two or more than two thermo-responsive diblock copolymers, which is still ongoing in our lab.

Acknowledgments

The financial support by National Science Foundation of China (№ 21274066 and 21474054) and PCSIRT (IRT1257) is gratefully acknowledged.

Notes and references

Key Laboratory of Functional Polymer Materials of the Ministry of Education, State Key Laboratory and Institute of Elemento-Organic Chemistry, Collaborative Innovation Center of Chemical Science and Engineering (Tianjin), Institute of Polymer Chemistry, Nankai University, Tianjin 300071, China.

**To whom correspondence should be addressed. E-mail: wqzhang@nankai.edu.cn, Tel: 86-22-23509794, Fax: 86-22-23503510.*

† Electronic Supplementary Information (ESI) available: Text showing Experimental procedures of the separation of the PNIPAM-*b*-PS/PDMAEMA-*b*-PS mixture, Scheme S1 showing the chemical structure of DMAEMA and CDTPA, Figure S1 showing the polymerization kinetics of the PNIPAM-TTC mediated dispersion polymerization and the PDMAEMA-TTC mediated dispersion polymerization, Figure S2 showing the ln([M]0/[M])-time plots of the two macro-RAFT agents co-mediated dispersion polymerization, Figure S3 showing the typical PNIPAM-*b*-PS/PDMAEMA-*b*-PS mixture prepared at 4 h before and after separation, Figure S4 showing the TEM images of the $PNIPAM_{92}$-*b*-PS_{275} nanoparticles and the $PDMAEMA_{61}$-*b*-PS_{265} nanoparticles, and Figure S5 showing the transmittance versus temperature plots for the aqueous solution of $PNIPAM_{92}$-TTC and $PDMAEMA_{61}$-TTC. Details of any supplementary information available should be included here. See DOI: 10.1039/b000000x/.

1 D. Roy, W. L. A. Brooks, B. S. Sumerlin, *Chem. Soc. Rev.* 2013, **42**, 7214-7243.
2 V. Aseyev, H. Tenhu, F. M. Winnik, *Adv. Polym. Sci.* 2011, **242**, 29-89.
3 Q. Li, F. Huo, Y. Cui, C. Gao, S. Li, W. Zhang, *J. Polym. Sci. Part A: Polym. Chem.* 2014, **52**, 2266-2278.
4 Q. Li, C. Gao, S. Li, F. Huo, W. Zhang, *Polym. Chem.* 2014, **5**, 2961-2972.
5 J. Xu, S. Luo, W. Shi, S. Liu, *Langmuir* 2006, **22**, 989-997.
6 H. Wei, S. Perrier, S. Dehn, R. Ravarian, F. Dehghani, *Soft Matter* 2012, **8**, 9526-9528.
7 C. Li, N. J. Buurma, I. Haq, C. Turner, S. P. Armes, V. Castelletto, I. W. Hamley, A. L. Lewis, *Langmuir* 2005, **21**, 11026-11033.
8 F. D. Jochum, P. J. Roth, D. Kessler, P. Theato, *Biomacromolecules* 2010, **11**, 2432-2439.
9 P. J. Roth, T. P. Davis, A. B. Lowe, *Macromolecules* 2012, **45**, 3221-3230.
10 H. -N. Lee, Z. Bai, N. Newell, T. P. Lodge, *Macromolecules* 2010, **43**, 9522-9528.
11 S. Li, F. Huo, Q. Li , C. Gao , Y. Su, W. Zhang, *Polym. Chem.* 2014, **5,** 3910-3918.
12 M. Dan, Y. Su, X. Xiao, S. Li, W. Zhang, *Macromolecules* 2013, **46**, 3137-3146.
13 Y. Su, Q. Li, S. Li, M. Dan, F. Huo, W. Zhang, *Polymer* 2014, **55**, 1955-1963.
14 A. Hanisch, A. H. Gröschel, M. Förtsch, M. Drechsler, H. Jinnai, T. M. Ruhland, F. H. Schacher, A. H. E. Müller, *ACS Nano* 2013, **7**, 4030-4041.
15 C. Liu, M. A. Hillmyer, T. P. Lodge, *Langmuir* 2008, **24**, 12001-12009.
16 J. Mao, P. Ni, Y. Mai, D. Yan, *Langmuir* 2007, **23**, 5127-5134.
17 L. Wang, R. Xu, Z. Wang, X. He, *Soft Matter* 2012, **8**, 11462-11470.
18 Z. Ge, S. Liu, *Macromol. Rapid Commun.* 2009, **30**, 1523-1532.
19 Y. Zhang, H. Liu, J. Hu, C. Li, S. Liu, *Macromol. Rapid Commun.* 2009, **30**, 941-947.
20 N. J. Warren, O. O. Mykhaylyk, D. Mahmood, A. J. Ryan, S. P. Armes, *J. Am. Chem. Soc.* 2014, **136**, 1023-1033.
21 L. A. Fielding, J. A. Lane, M. J. Derry, O. O. Mykhaylyk, S. P. Armes, *J. Am. Chem. Soc.* 2014, **136**, 5790-5798.
22 M. Topuzogullari, V. Bulmus, E. Dalgakiran, S. Dincer, *Polymer* 2014, **55**, 525-534.
23 I. Berndt, J. S. Pedersen, W. Richtering, *Angew. Chem. Int . Ed.* 2006, **45**, 1737-1741.
24 L. Cheng, X. Lin, F. Wang, B. Liu, J. Zhou, J. Li, W. Li, *Macromolecules* 2013, **46**, 8644-8648.
25 X. Liu, H. Gao, F. Huang, X. Pei, Y. An, Z. Zhang, L. Shi, *Polymer* 2013, **54**, 3633-3640.
26 M. Štěpánek, K. Podhájecká, E. Tesarová, K. Procházka, Z. Tuzar, W. Brown, *Langmuir* 2001, **17**, 4240-4244.
27 F. J. Esselink, E. E. Dormidontova, G. Hadziioannou, *Macromolecules* 1998, **31**, 4873-4878.
28 R. Zheng, G. Liu, X. Yan, *J. Am. Chem. Soc.* 2005, **127**, 15358-15359.
29 F. Schacher, E. Betthausen, A. Walther, H. Schmalz, D. V. Pergushov, A. H. E. Müller, *ACS Nano* 2009, **3**, 2095-2102.
30 E. W. Price, Y. Guo, C. -W. Wang, M. G. Moffitt, *Langmuir* 2009, **25**, 6398-6406.
31 D. A. Christian, A. Tian, W. G. Ellenbroek, I. Levental, K. Rajagopal, P. A. Janmey, A. J. Liu, T. Baumgart, D. E. Discher, *Nature Mater.* 2009, **8,** 843-849.
32 J. Zhu, R. C. Hayward, *Macromolecules* 2008, **41**, 7794-7797.
33 J. -F. Gohy, N. Lefèvre, C. D'Haese, S. Hoeppener, U. S. Schubert, G. Kostov, B. Améduri, *Polym. Chem.* 2011, **2**, 328-332.
34 G. Srinivas, J. W. Pitera, *Nano Lett.* 2008, **8**, 611-618.
35 T. Nicolai, O. Colombani, C. Chassenieux, *Soft Matter* 2010, **6**, 3111-3118.
36 Z. Li, M. A. Hillmyer, T. P. Lodge, *Macromolecules* 2006, **39**, 765-771.
37 D. J. Pochan, J. Zhu, K. Zhang, K. L. Wooley, C. Miesch, T. Emrick, *Soft Matter* 2011, **7**, 2500-2506.
38 S. I. Yoo, B. -H. Sohn, W.-C. Zin, J. C. Jung, C. Park, *Macromolecules* 2007, **40**, 8323-8328.
39 B. Charleux, G. Delaittre, J. Rieger, F. D'Agosto, *Macromolecules* 2012, **45**, 6753-6765.
40 J.-T. Sun, C.-Y. Hong C.-Y. Pan, *Soft Matter* 2012, **8**, 7753-7767.
41 N. J. Warren, S. P. Armes, *J. Am. Chem. Soc.* 2014, DOI: 10.1021/ja502843f.
42 M. Semsarilar, V. Ladmiral, A. Blanazs, S. P. Armes, *Langmuir* 2012, **28**, 914-922.
43 A. Blanazs, J. Madsen, G. Battaglia, A. J. Ryan, S. P. Armes, *J. Am. Chem. Soc.* 2011, **133**, 16581-16587.
44 X. Wang, S. Li, Y. Su, F. Huo, W. Zhang, *J. Polym. Sci. Part A: Polym. Chem.* 2013, **51**, 2188-2198.
45 J. Xu, X. Xiao, Y. Zhang, W. Zhang, P. Sun, *J. Polym. Sci. Part A: Polym. Chem.* 2013, **51**, 1147-1161.
46 Y. Su, X. Xiao, S. Li, M. Dan, X. Wan, W. Zhang, *Polym. Chem.* 2014, **5**, 578-587.
47 M. Dan, F. Huo, X. Zhang, X. Wang, W. Zhang, *J. Polym. Sci. Part A: Polym. Chem.* 2013, **51**, 1573-1584.
48 X. Xiao, S. He, M. Dan, Y. Su, F. Huo, W. Zhang, *J. Polym. Sci. Part A: Polym. Chem.* 2013, **51**, 3177-3190.
49 X. Wang, J. Xu, Y. Zhang, W. Zhang, *J. Polym. Sci. Part A: Polym. Chem.* 2012, **50**, 2452-2462.
50 Y. Pei, N. C. Dharsana, J. A. van Hensbergen, R. P. Burford, P. J. Roth, A. B. Lowe, *Soft Matter* 2014, **10**, 5787-5796.
51 G. Moad, Y. K. Chong, A. Postma, E. Rizzardo, S. H. Thang, *Polymer* 2005, **46**, 8458-8468.
52 A. P. Narrainen, A. Pascual, D. M. Haddleton, *J. Polym. Sci. Part A: Polym. Chem.* 2002, **40**, 439-450.
53 H. de Brouwer, M. A. J. Schellekens, B. Klumperman, M. J. Monteiro, A. L. German, *J. Polym. Sci. Part A: Polym. Chem.* 2000, **38**, 3596-3603.

54 C. Yang, J. N. Kizhakkedathu, D. E. Brooks, F. Jin, C. Wu, *J. Phys. Chem. B* 2004, **108**, 18479-18484.
55 A. H. Gröschel, F. H. Schacher, H. Schmalz, O. V. Borisov, E. B. Zhulina, A. Walther, A. H. E. Müller, *Nature Commun.* 2012, **3**, 1-10.